A NEW CHITOSAN BIOPOLYMER DERIVATIVE FOR THE REMOVAL OF COPPER (II) AND LEAD (II) FROM AQUEOUS SOLUTIONS: SYNTHESIS, CHARACTERIZATION AND ADSORPTION STUDIES

K. Balakrishna Prabhu[a,b], M. B. Saidutta[b], Arun M. Isloor[c*], Girish Kamath[a]

*Corresponding author
isloor@yahoo.com

[a]Department of Chemical Engineering, Manipal Institute of Technology, Manipal, India
[b]Department of Chemical Engineering, National Institute of Technology Karnataka, Surathkal, Mangaluru, India
[c]Department of Chemistry, National Institute of Technology Karnataka, Surathkal, Mangaluru, India

Graphical abstract

Chitosan

Ligand-L

CTSL-Pb and CTSL-Cu

Chitosan derivative (CTSL)

Abstract

A new chitosan derivative was prepared by grafting a ligand [3-(4methoxyphenyl)-1H-pyrazole-4-carbaldehyde] to chitosan by a Schiff base reaction. The chitosan-ligand derivative (CTSL) was characterized by spectral studies (FT-IR, ^{13}C NMR, XRD) and scanning electronic microscope. The suitability of CTSL as an adsorbent for the removal of two metals viz. Cu (II) and Pb (II) was studied by conducting equilibrium, kinetic and thermodynamic studies. Experimental data obtained in equilibrium studies were analyzed for Langmuir, Freundlich, and Redlich-Peterson isotherms. The maximum monolayer adsorption capacity obtained for the two metals were CTSL-Cu (40.62 mg/g) and CTSL-Pb (71.99 mg/g). The data obtained from the kinetic study was analyzed with three models viz. pseudo-first order, pseudo-second order and intraparticle diffusion models. The pseudo-second-order rate equation fitted the experimental data very well. Thermodynamic parameters ΔG, ΔH and ΔS were determined. The sorption operation was feasible, exothermic and accompanied with a positive increase in entropy. The metal interactions with the adsorbent were attributed to the hydroxyl, imine and the amine groups present in the synthesized derivative.

Keywords: Chitosan derivative, adsorption, Schiff base, pyrazole ring, metal removal

1.0 INTRODUCTION

Pollution of environmental waters due to the discharge of heavy metals (such as Cu, Pb) is a growing concern. Possible sources of the heavy metal release into aquatic media are the industries such as mining, electroplating, fabrication, leather tanning, fertilizer, textile dyes, printing, and acid battery manufacturing. Other causes for the heavy metal contamination include natural erosion, waste discharge, atmospheric depositions, landfills, pesticide application to crops and additional anthropogenic activities [1, 2]

Among the major technologies in use for the elimination of heavy metals from industrial wastewaters, adsorption techniques are finding widespread acceptance due to their simplicity, potential of

regeneration and low cost [3]. Adsorption techniques can be successfully employed for the elimination of heavy metals present in dilute solutions [2].

Of late, sorption techniques that use chitosan and its derivatives have attracted a lot of research attention. Chitosan is easily obtained from the deacetylation of chitin which is a key constituent of crustacean waste shells. Chitin is also one of the most abundant biopolymers in the natural world [4]. Chitosan has been established as an effective agent for the uptake of transition metal ions present in wastewater, which is chiefly attributed to its amino group [5]. Chitosan has many attractive attributes that are well-recognized viz: biocompatibility, biodegradability, renewability, hydrophilicity, bioactivity, and non-toxicity [6]. Recently many modified chitosan derivatives have been synthesized and investigated for adsorption applications [7, 8, 9]. The presence of amino groups in the chemical structure of chitosan permits reactions with several substituents, with the possibility of creating a variety of modified biopolymers [10]. Schiff bases are a class of modified biopolymers, having an imine group (–RC=N–), obtained by reacting the amino groups (NH$_2$) of chitosan with a carbonyl group (>C=O) of an aldehyde or ketone [11,12].

Even though many modifications of chitosan have been studied, to the knowledge of the authors, adsorptive metal removal studies with chitosan grafted with ligands having pyrazole ring have not been reported. The pyrazole ring provides additional nitrogen atoms in the modified product. In the present study, a novel derivative of chitosan (CTSL) was synthesized by grafting of the pyrazole ring bearing ligand 3-(4-methoxyphenyl)-1H-pyrazole-4-carbaldehyde (L) to the chitosan (CTS) backbone by a Schiff base reaction. It is well known that both nitrogen and oxygen atoms have the ability to chelate cations by transferring the lone pair of electrons to the metal ion [13]. The addition of the new functional groups was expected to enhance the ability of CTSL for the uptake of the metal ions owing to the extra nitrogen bearing groups of the added moiety.

2.0 METHODOLOGY

2.1 Materials

The chitosan used for this research, in powder form (30 mesh), with 90% deacetylation and average molecular weight 5.0×10^5 Da, was procured from Seafresh Industry Public Co. Ltd. Thailand. The biopolymer was used as received. 4-methoxy acetophenone (Merck KGaA, Germany) and semicarbazide hydrochloride (Merck Schuchardt OHG, Germany) and all other chemicals and solvents used were of AR grade.

Solutions of Pb (II) and Cu (II) were prepared by dissolving Pb(NO$_3$)$_2$ (NICE chemicals, Cochin) and CuSO$_4$.5H$_2$O (Merck, India) respectively, in double distilled water.

2.2 Synthesis of CTSL

The ligand L (3-(4-methoxyphenyl)-1H-pyrazole-4-carbaldehyde) was synthesized from 4-methoxyacetophenone and semicarbazide hydrochloride according to a previously reported procedure [14]. To prepare the CTSL, chitosan in powder form (3 g) was taken with 1 % acetic acid (76 mL) and kept under stirring at room temperature for one hour. Further, the thick solution was diluted by adding methanol (350 mL) and stirred for an additional 16 h. To this, ligand (L) (6 g, dissolved in 60 mL of chloroform) was added over a period of 10 min at room temperature. Agitation was continued for a further period of 16 h at room temperature (Figure 1).
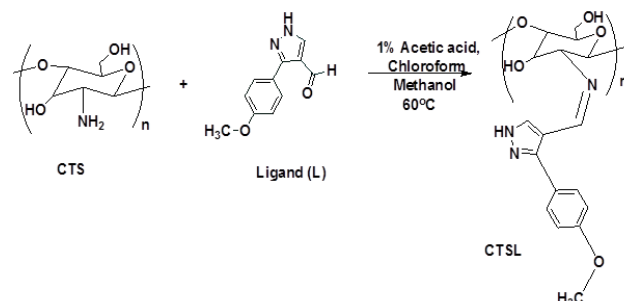
Figure 1 Synthesis of Chitosan-Ligand derivative (CTSL)

The mixture was then heated to 60°C and refluxed for 18 h under agitation, after which it was cooled to room temperature; chloroform (75 mL) was added to the reaction mass and stirred for 10 min to remove any unreacted components. The yellow mass (CTSL) obtained was filtered, washed with chloroform and dried at 50°C. (Yield: 6 g, 93.3 %)

2.3 Characterization

FT-IR RX-1 model by SHIMADZU was used to record the Fourier transformed infrared spectra on KBr pellets. \$^{13}$C NMR spectra were recorded on 400 MHz Solid state NMR spectrometer. ^{1}H NMR spectrum was recorded by 400 MHz Bruker Biospin NMR spectrometer. Thermo-Scientific iCE 3000 series atomic absorption spectrometer was utilized to measure the metal ion concentrations. Rigaku Miniflux-600 X-ray powder diffractometer was used for X-ray diffraction studies. Jeol JED 2300 Analysis Station scanning electron microscope was used to record the surface morphologies of the samples. Systronics digital pH meter 335 was used to measure the pH.

2.4 Adsorption Experiments

2.4.1 ph Studies

Cu (II) and Pb (II) solutions of concentration100 mg/L were prepared at the required pH values (2 to 8) and 25 mL of each was taken and agitated with 100 mg of the adsorbent for duration of 24 h in an incubator

shaker at 30°C and 150 rpm. After adsorption, samples were drawn using a syringe and filtered with syringe filter of 0.2-micron size. They were then diluted and analyzed by atomic absorption spectrometer (AAS). The adsorption capacity was then determined using Equation 1[6].

$$Q_e = \frac{(C_o - C_e)V}{W} \qquad (1)$$

Where 'Qe' is the equilibrium adsorption capacity of the CTSL (mg/g of adsorbent), 'Co' and 'Ce' are the initial and equilibrium concentrations of the solute (mg/L) respectively, 'V' is the volume of the solution (mL) and 'W' is the mass of the sorbent (g).

2.4.2 Adsorption Equilibrium Studies

25 mL of solutions having metal ions Cu (II) and Pb (II) with initial concentrations in the range of 25 mg/L to 1000 mg/L at the optimum pH for adsorption were taken in Erlenmeyer flasks and to each, 50 mg of CTSL was added. The samples were then kept under agitation for 24h in an incubator shaker at 150 rpm and 30°C. Samples were drawn, filtered, diluted and their concentrations were analyzed by AAS. The extent of metal ions removed was determined using Equation 1.

2.4.3 Adsorption Kinetic Studies

The kinetic study was conducted by taking 125 mL of the metal ion solutions having an initial concentration of 100 mg/L at the optimum pH corresponding to the respective metal ion with an adsorbent dosage of 250 mg. The solutions were shaken for 24 h at constant temperature and aliquots were drawn at fixed time intervals, filtered, diluted and their concentrations were analyzed by AAS. The quantity adsorbed ('Qt', mg/g) at time 't' (min) was calculated by Equation 2 [15].

$$Q_t = \frac{(C_o - C_t)V}{W} \qquad (2)$$

in which 'Ct' (mg/L) is the concentration of the metal ion at time 't' (min).

2.4.4 Adsorption Thermodynamic Studies

Thermodynamic studies were performed with several initial concentrations of adsorbate falling in the range of 10 mg/L - 250 mg/L. The experimental temperature was between 283.15 K and 323.15 K. Volume of each metal ion solution taken was 25 mL with an adsorbent dose of 50 mg.

3.0 RESULTS AND DISCUSSIONS

3.1 Characterization of the Ligand (L)

The ^{1}H NMR spectrum of the ligand exhibited the following peaks. ^{1}H NMR (DMSO-d6) δ (ppm): 13.651

(1 H, Pyrazole NH), 9.873 (1 H, Aldehyde), 7.080-7.787 (4 H, Ar. Ring), 8.290 (1 H, Pyrazole 5H), 3.825 (3 H, Methoxy).

3.2 Characterization of CTSL:

The scanning electron micrographs of the pure chitosan and CTSL surface are presented in Figure 2. The morphology exhibits the decreased surface flakiness in CTSL as compared to CTS. The sturdy and bulky appearance of CTSL particles as compared to flaky and flat particles of CTS is also discernible from the micrograph.
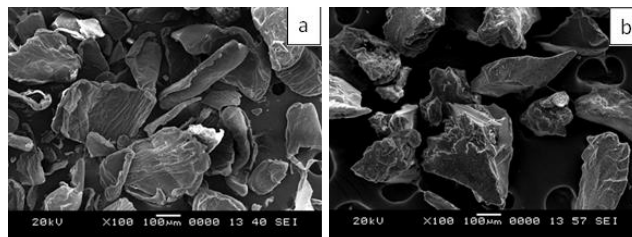
Figure 2 Scanning electron micrographs of a) CTS b) CTSL

The solid state ^{13}C NMR spectra for chitosan and CTSL are shown in Figure 3 a and b. The ^{13}C NMR of CTSL shows a peak at 161.4 ppm which is assigned to imine (>C=N) formed during the Schiff reaction [16]. The aromatic rings were represented between 110 ppm and 131.4 ppm. The appearance of new peaks in the aromatic region and the changes in peak intensity for CTSL when compared to chitosan confirms the successful grafting of the ligand on chitosan [17].
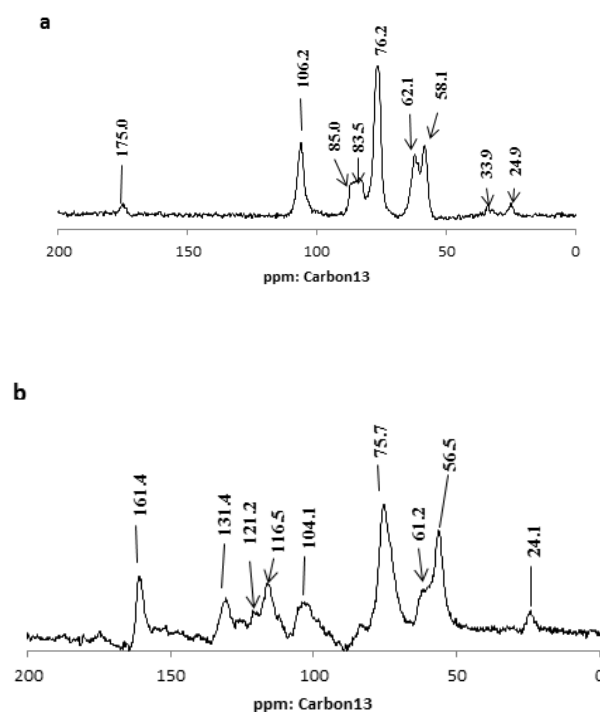
Figure 3 Solid state ^{13}C NMR spectra of a) Chitosan and b) CTSL

The FT-IR spectra for pure chitosan and CTSL are shown in Figure 4 a and 4 b respectively. The major bands for pure chitosan are as follows: 3400cm^{-1} to 3630 cm^{-1} (br, O-H and NH_2 stretching vibrations); 2885 cm^{-1} (-CH) stretching vibration in (-CH) and (-CH_2); 1654 cm^{-1} (>C=O) stretching vibration of remaining acetyl units of CTS-NHAc; 1581cm^{-1} amide II band of CTS-NHAc; 1373 cm^{-1} (-CH) symmetric bending vibration in (-CHOH-); 1153 cm^{-1} stretching vibration in (C-O-C bridge); 1083 cm^{-1} (s, -C-O) stretching vibration in (-COH); 891 cm^{-1} (C-H) out of plane bending; 663 cm-1 (N-H) wagging vibrations [18].

The FT-IR pattern for CTSL has a broad band at 3548-3687 cm^{-1} ascribed to the (-OH) stretch. The band at 1674 cm^{-1} is due to the presence of (>C=O) stretching vibrations of acetyl units of CTS-NHAc. The splitting of the band at 1632 cm^{-1} is attributed to the imine (>C=N-) stretch. The peak at 1515 cm^{-1} is assigned to NH bending. The peak at 1250 cm^{-1} is due to alkyl-aryl (C-O) stretch. The two peaks at 1068 cm^{-1} and 1010 cm^{-1} are assigned to the C-O stretching vibrations in C-O-H of the secondary and primary alcohols respectively. The peak at 833 cm^{-1} is attributed to aromatic (-CH) out of plane bending. The peak at 644 cm^{-1} is assigned to NH wagging [17].
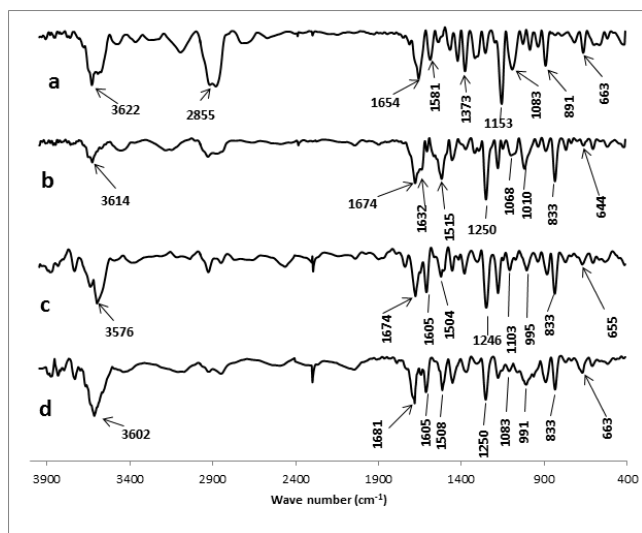
Figure 4 FT-IR spectra of a) CTS b) CTSL c) CTSL-Pb d) CTSL-Cu

The XRD pattern of CTS (Figure 5 a) shows the characteristic peaks around 2Ө=10°, 2Ө=19° and 2Ө=21° [20]. The disappearance of the peak at 2Ө=10° in the spectrum for CTSL (Figure 5 b) attributed to (-NH_2) group is further evidence of the Schiff base reaction at the (-NH_2) group [21]. The decrease in the intensity and broadening of the peaks in the section around 2Ө=20° for CTSL indicates the decrease in crystallinity and increased amorphous nature of CTSL as compared to pure CTS [6].
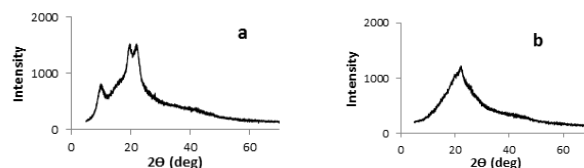
Figure 5 a) XRD spectrum of chitosan (CTS) b) XRD spectrum of CTSL

3.3 Effect of pH

The pH effect was studied within the pH range of 2-8 since precipitation of metal ions as hydroxides can occur at higher pH values [22]. Maximum percentage removal obtained for Pb (II) was 98%; there was very little (±2%) variation in % removal within the pH range of 4-8 (Figure 6). The maximum percentage removal obtained for Cu (II) was 61%. Based on these results, the equilibrium, kinetic and thermodynamic studies were conducted with the optimum pH of 4 for Pb (II), and pH of 7 for Cu (II) removal. The steep fall in percentage removal of metal ions in the pH range 2-4 is explained as follows: At pH < 4, protonation occurs at the nitrogen atoms of CTSL which results in positive charges on the surface of the adsorbent causing electrostatic repulsion with the positively charged Cu (II) and Pb (II) ions. However, for pH > 4, the adsorption sites get deprotonated, when metal binding can occur by chelation, leading to increasing adsorption efficiency [23]. The adsorbent appeared to be stable in the pH range of 3-8. However, there was evidence of its instability by fragmentation at pH < 3 which resulted in a catastrophic drop in adsorption efficiency.
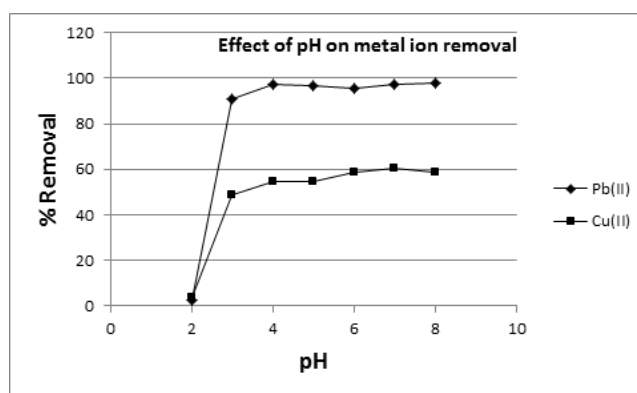
Figure 6 Effect of pH on % removal (Initial conc. = 100mg/L; T= 303 K; Ads. Dose= 4g/L; Stirring speed= 150 rpm; t = 24 h)

3.4 Adsorption Equilibrium

In order to establish the applicable adsorption equilibrium isotherm, three models viz. Langmuir, Freundlich, and Redlich-Peterson were employed. A comprehensive list of adsorption isotherms with their fundamental attributes and mathematical derivations have been presented in a review article [24].

Langmuir adsorption isotherm [24] assumes monolayer adsorption with all adsorption sites being equivalent. The equation for the Langmuir isotherm is as shown in Equation 3:

$$Q_e = \frac{Q_o b C_e}{b C_e + 1} \quad (3)$$

where, 'Q_e' and 'Q_o' represent equilibrium and maximum monolayer adsorption capacities (mg/g) respectively, 'b' is the Langmuir constant (L/mg), and 'C_e' is the equilibrium adsorbate concentration (mg/L). The basic features of the Langmuir isotherm can be elaborated by a dimensionless number 'R_L' [22].

$$R_L = \frac{1}{1 + b C_o} \quad (4)$$

'R_L', called the separation parameter, gives insight into the nature of adsorption: adsorption is variously, irreversible ($R_L = 0$), favorable ($0 < R_L < 1$), linear ($R_L = 1$) and unfavorable ($R_L > 1$).

Freundlich isotherm [21] is an empirical model applied to multilayer adsorption with non-uniform surface reactivity and heat of adsorption on the adsorbent surface and is represented by:

$$Q_e = K_f C_e^{1/n} \quad (5)$$

in which 'K_f' stands for Freundlich adsorbent constant (mg/g) and 'n' the dimensionless Freundlich exponent related to the propensity for adsorption.

Many hybrid isotherms that combine aspects of both the Langmuir and Freundlich equations have also been proposed. Redlich-Peterson isotherm is one such isotherm which incorporates three parameters in the model. Redlich-Peterson isotherm [21] represents adsorption equilibria across a broad concentration span, has practical uses in homogeneous or heterogeneous systems owing to its adaptability. The mathematical form of this isotherm is given by Equation 6.

$$Q_e = \frac{K_R C_e}{1 + a_R C_e^{b_R}} \quad (6)$$

where, 'K_R' (L g^{-1}), 'a_R' (L mg^{-1}) and 'b_R' are parameters.

Non-linear analysis with minimization of the sum of squared errors method was employed with MICROSOFT EXCEL Solver add-in for fitting the Langmuir, Freundlich and Redlich-Peterson isotherm models. The results are tabulated in Table 1. The corresponding plots are as per Figure 7 and Figure 8. For the removal of Cu (II), Langmuir and Redlich-Peterson isotherm models gave better results ($r^2 = 0.962$ and 0.963 respectively) whereas for the removal of Pb (II), the Freundlich and Redlich-Peterson isotherm models were better ($r^2 = 0.927$ and 0.929 respectively). The maximum monolayer adsorption capacities (Q_o) were 40.62 mg/g for Cu (II) and 71.99 mg/g for Pb (II). The Langmuir separation factor R_L which was within 0-1 and the Freundlich

exponent (n) which was between 1 and 10 indicated that the adsorption was favorable [12]. It has been reported that values of b_R between 0 and 1 in the Redlich-Peterson model indicate a favorable adsorption, and the higher values may indicate a milder sorptive interaction between adsorbent and adsorbate [25]. The values obtained in this study for b_R - 0.984 for Cu (II), and 0.670 for Pb (II) - point towards adsorption being favorable.

Table 1 Equilibrium model parameters of adsorption of Cu (II) and Pb (II) ions on CTSL

Isotherm	Cu (II)	Pb (II)
Langmuir Isotherm		
Q_o (mg g^{-1})	40.62	71.985
b (L mg^{-1})	0.0161	0.011
r^2	0.962	0.891
R_L	0.71-0.0584	0.784-0.0833
Freundlich Isotherm		
K_f (mg g^{-1})	4.874	5.672
N	3.132	2.628
r^2	0.896	0.927
Redlich-Peterson Isotherm		
K_R (L g^{-1})	0.678	4.918
a_R (L mg^{-1})	0.018	0.619
b_R	0.984	0.670
r^2	0.963	0.929
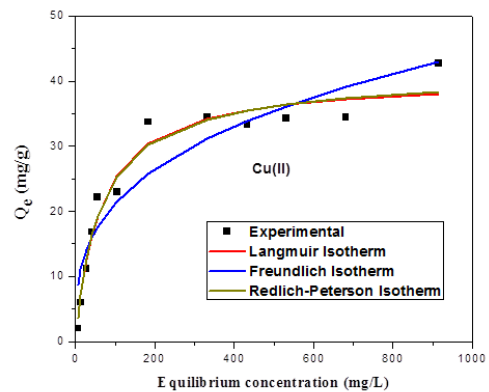
Figure 7 Plot of various adsorption isotherms to CTSL-Cu (II) adsorption data (Initial conc. = 100 mg/L; T = 303 K; pH 7; Ads. Dose= 2g/L; Stirring speed = 150 rpm; t = 24 h)
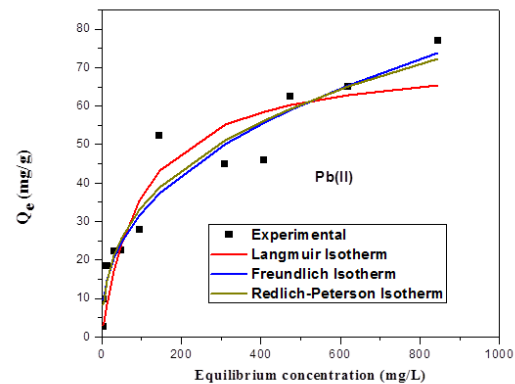
Figure 8 Plot of various adsorption isotherms to CTSL-Pb (II) adsorption data (Initial conc. = 100 mg/L; T = 303 K; pH 4; Ads. Dose= 2 g/L; Stirring speed= 150 rpm, t = 24 h)

3.5 Adsorption Kinetics

The kinetic analysis is of great importance in evaluating the rate at which the adsorbate is removed from the solution which helps determine the time for completion of the adsorption process. The kinetic parameters also help establish the size of the equipment of a fixed bed continuous contact system. Further, the kinetic data is of great value in understanding the underlying mechanism of sorption. Qiu *et al.* [26] have published a review article of the kinetic models used in adsorption systems.

In order to determine the adsorption kinetics of the metal ions uptake by modified chitosan adsorbents, three kinetic models have been widely employed. The pseudo-first order rate equation of Lagergren has the mathematical form as given in Equation 7 [26].

$$\ln(Q_e - Q_t) = \ln(Q_e) - k_1 t \tag{7}$$

where 'Q_e' and 'Q_t' represent the quantity adsorbed (mg/g) at equilibrium and time 't' (min) respectively. 'k_1' is the pseudo-first order adsorption rate constant (min^{-1}).

The pseudo-second-order rate equation is expressed as given in Equation 8 [26].

$$\frac{t}{Q_t} = \frac{t}{Q_e} + \frac{1}{k_2 Q_e^2} \tag{8}$$

where 'Q_e' and 'Q_t' represent the quantity adsorbed (mg/g) at equilibrium and time 't' (min) respectively, and 'k_2' is the adsorption rate constant ($g\ mg^{-1}min^{-1}$).

In some sorption systems, the amount of adsorbate removed varies almost linearly with the square root of the time of contact. This phenomenon is described by the Weber-Morris model given by Equation 9 [26].

$$Q_t = K_{id} t^{\frac{1}{2}} + C \tag{9}$$

where 'K_{id}' is the intraparticle diffusion rate constant ($mg\ g^{-1}.min^{-\frac{1}{2}}$) and 'C' is the intercept ($mg\ g^{-1}$). This model is applicable if the adsorption is governed by pore diffusion in the particles and convective diffusion in the solution.

The results of the kinetic study are tabulated in Table 2. Among the three models, the pseudo-second-order model was found to best represent the adsorption kinetics for the metal ions Cu (II) and Pb (II) (Figure 9 and Figure 10). Very high values of correlation coefficient are obtained for pseudo-second-order model (0.9942 for Cu (II) and 0.9991for Pb (II)) indicates that chemisorption may be the rate controlling step for the metal removal [27].

Table 2 Comparison of kinetic model parameters for Cu (II) and Pb (II)

Kinetic Model	Cu (II)	Pb (II)
Pseudo-first-order		
$Q_{e\ calc}$ (mg g^{-1})	24.293	27.871
$Q_{e\ expt.}$ (mg g^{-1})	32.418	48.302
k_1 (min^{-1})	0.0024	0.0207
r^2	0.9438	0.8793
Pseudo-second-order		
$Q_{e\ calc.}$ (mg g^{-1})	32.415	47.619
$Q_{e\ expt.}$ (mg g^{-1})	32.418	48.302
k_2 (g $mg^{-1}min^{-1}$)	0.00034	0.0014
r^2	0.9942	0.9991
Weber-Morris		
K_{id} (mg $g^{-1}min^{-½}$)	0.8632	3.357
C (mg g^{-1})	4.6748	13.529
r^2	0.9142	0.8078
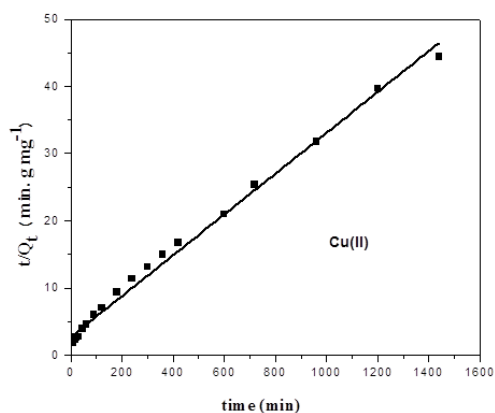
Figure 9 Pseudo-second order model for CTSL-Cu (II) (Initial conc. = 100 mg/L; T= 303 K; pH 7; Ads. Dose= 2 g/L; Stirring speed= 150 rpm)
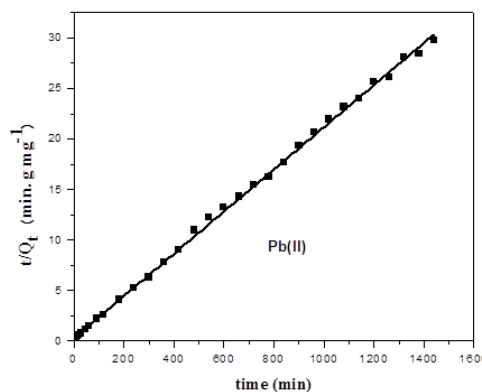
Figure 10 Pseudo-second order model for CTSL-Pb (II) (Initial conc. = 100 mg/L; T= 303 K; pH 4; Ads. Dose= 2 g/L; Stirring speed= 150 rpm)

3.6 Adsorption Thermodynamics

The feasibility of adsorption is governed by Gibb's free energy change (ΔG). Negative values of ΔG means the sorption occurs spontaneously. The Gibb's free energy change was determined employing the thermodynamic equilibrium constant 'K_o' [19].

$$K_o = \frac{a_s}{a_e} = \frac{v_s Q_e}{v_e C_e} \qquad (10)$$

where 'a_s' is the activity of the adsorbed metal ion, 'a_e' is the activity of the metal ion in the solution at equilibrium, 'v_s' and 'v_e' represent activity coefficients of the adsorbate on the adsorbent surface and the equilibrated solution. 'Q_e' and 'C_e' represent surface concentrations of metal ions (mmol g^{-1}) and concentration of metal ions in solution at equilibrium (mmol mL^{-1}) respectively. At vanishing concentrations of the metal ion in the solution, both the activity coefficients 'v_s' and 'v_e' approach unity [28].

$$\lim_{Q_e \to 0} \frac{a_s}{a_e} = \frac{Q_e}{C_e} = K_o \qquad (11)$$

'K_o' may be obtained by plotting a straight line of $\ln(Q_e/C_e)$ versus Q_e and extending Q_e to zero. The standard free energy change (ΔG°) can be determined from the Van't Hoff Equation.

$$\Delta G^\circ = -RT \ln K_o \qquad (12)$$

where R is the universal gas constant (8.314 J/mol.K), T is the temperature (K).

The standard change in enthalpy (ΔH°) and standard change in entropy (ΔS°) are then related to the standard change in Gibbs free energy, (ΔG°) through Equation13:

$$\Delta G^\circ = \Delta H^\circ - T\Delta S^\circ \qquad (13)$$

From which follows the Equation 14

$$\ln K_o = \frac{\Delta S^\circ}{R} - \frac{\Delta H^\circ}{RT} \qquad (14)$$

'K_o' was obtained from Equation 11 and the values of ΔH° and ΔS° were determined as per Equation 14 from the slope and intercept of the plot of ln K_o v/s 1/T respectively.

The results are tabulated in Table 3. ΔG° of adsorption for both the metals studied had negative values which suggest that the adsorption process was spontaneous.

Table 3 Results of Thermodynamic study for the adsorption Cu (II) and Pb (II) ions onto CTSL

Temperature (K)	K_o	ΔG° (kJ.mol^{-1})	ΔH° (kJ.mol^{-1})	ΔS° (J.mol^{-1}.K^{-1})
Cu (II)				
283.15	210.38	12.585	25.22	133.8
293.15	301.42	13.906		
303.15	494.43	15.627		
313.15	562.11	16.477		
323.15	811.27	17.988		
Pb (II)				
283.15	792.59	15.706	14.87	107.80
293.15	980.24	16.779		
303.15	1471.44	18.375		
313.15	732.53	17.166		
323.15	2399.22	20.900		

The values for enthalpy change (ΔH°) for both Pb (II) and Cu (II) were positive implying the adsorption process was endothermic. Adsorption was favored by an increase in temperature in the range of 10 °C to 50 °C. The net entropy changes (ΔS°) for sorption of both the metals were also positive, signifying net disorderliness increased post adsorption.

3.7 Post-Adsorption CTSL Characterization

The FT-IR spectra of CTSL and CTSL metal complexes are depicted in Figure 4 b, c, and d. The comparison of the spectra reveals the following differences: The broad peak in CTSL at wave number 3614 cm^{-1} due to (OH) stretching shifts to 3576 cm^{-1} for CTSL-Cu and 3602 cm^{-1} for CTSL-Pb. Further, a peak in CTSL around 1632 cm^{-1} which is attributed to imine group (>C=N-) shifts to 1605 cm^{-1} in the case of both CTSL-Pb and CTSL-Cu. The peak at 1515 cm^{-1} due to NH bending shifts to 1504 cm^{-1} for CTSL-Pb and to 1508 cm^{-1} for CTSL-Cu. The peak at 1068 cm^{-1} due to the C-O stretching vibrations in the secondary alcohol C-O-H is shifted to 1103 cm^{-1} (CTSL-Pb) and 1083 cm^{-1} (CTSL-Cu); the peak at 1010 cm^{-1} due to C-O stretching vibrations in the primary alcohol C-O-H is shifted to 995 cm^{-1} (CTSL-Pb) and 991 cm^{-1} (CTSL-Cu). The peak due to secondary NH wagging vibrations at 644 cm^{-1} is shifted to 655 cm^{-1} (CTSL-Pb) and 663 cm^{-1} (CTSL-Cu)[17, 29]. No significant shift was observed at the wavenumber 1250 cm^{-1} corresponding to the alkyl-aryl C-O linkage. Based on these considerations, it is postulated that probably the OH, imine and NH groups were responsible for metal adsorption process. Proposed mechanisms of metal (Cu (II) and Pb(II)) removal is shown in Figure 11 a and b.
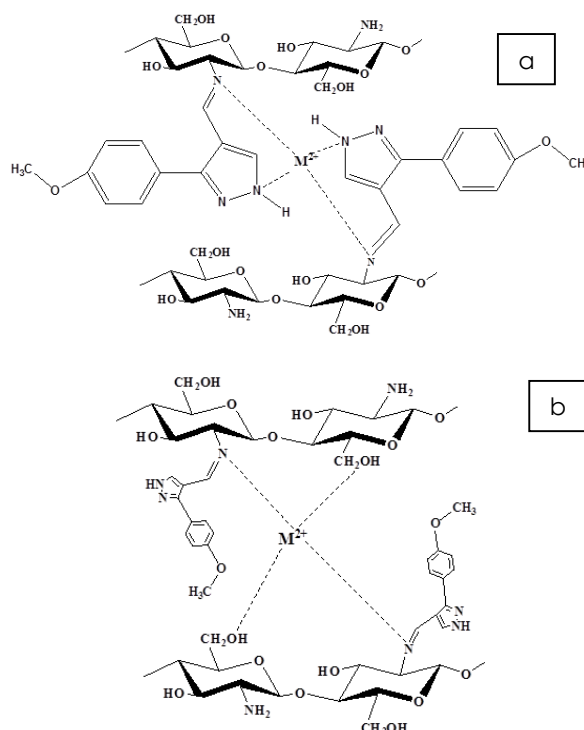
Figure 11 a, b Proposed mechanisms of adsorbate uptake. (M^{2+} = Pb (II) or Cu (II))

4.0 CONCLUSIONS

A new chitosan derivative was made by grafting chitosan with ligand bearing pyrazole ring, employing a Schiff base reaction. It was characterized by solid state ^{13}C NMR, FT-IR, SEM and powder XRD spectra, and its effectiveness as an adsorbent investigated by equilibrium, kinetic and thermodynamic studies.

Adsorption of Cu (II) and Pb (II) was favored at pH 4 to 7. For Cu (II), Redlich-Peterson and Langmuir Equilibrium isotherms fitted the experimental data well; for Pb (II) the Redlich-Peterson and Freundlich isotherms gave a better fit. Maximum monolayer adsorption capacities Q_o recorded for the sorption was CTSL-Cu (40.62 mg.g^{-1}, 0.639 mmol.g^{-1}) and CTSL-Pb (71.99 mg.g^{-1}, 0.347 mmol.g^{-1}). The Langmuir separation factor R_L (within 0-1) and the Freundlich isotherm exponent n (within 1-10) points to a favorable adsorption process.

The pseudo-second order kinetic model gave better agreement with experimental values for both Cu (II) and Pb (II) (r^2 = 0.994 and 0.999 respectively). The thermodynamic study indicated the spontaneous nature of adsorption. Adsorption of both Cu (II) and Pb (II) was endothermic and favored at higher temperatures. The ΔH^o values for metal removal were 25.22 kJ/mol for Cu (II) and 14.87 kJ/mol for Pb (II). The net entropy changes (ΔS^o) for sorption of both the metal ions were positive indicating that the net disorderliness increased post adsorption. It is suggested that the hydroxyl, imine and NH groups were responsible for metal adsorption process.

Based on the above results, it can be concluded that the synthesized derivative was very effective in the sorption Cu (II) and Pb (II) ions from aqueous solutions.

Acknowledgement

References

[1] Monier, M., Ayad, D. M., Wei, Y., and Sarhan, A. A. 2010. Adsorption of Cu (II), Co (II), and Ni (II) Ions by Modified Magnetic Chitosan Chelating Resin. *Journal of Hazardous Materials.* 177: 962-970.

[2] Wang, J., and Chen, C. 2009. Biosorbents for Heavy Metals Removal and Their Future. *Biotechnology Advances.* 27: 195-226.

[3] Choi, J. W., Chung, S. G., Hong, S. W., Kim, D. J., and Lee, D. J. 2012. Development of an Environmentally Friendly Adsorbent for the Removal of Toxic Heavy Metals from Aqueous Solution. *Water, Air and Soil Pollution.* 223: 1837-1846.

[4] Wu, F. C., Tseng, R. L., and Juang, R. S. 2010. A Review and Experimental Verification of Using Chitosan and Its Derivatives as Adsorbents for Selected Heavy Metals. *Journal of Environmental Management.* 91: 798-806.

[5] Guibal, E. 2004. Interactions of Metal Ions with Chitosan-based Sorbents: A Review. *Separation and Purification Technology.* 38: 43-74.

[6] Krishnapriya, K. R., and Kandaswamy, M. 2010. A New Chitosan Biopolymer Derivative as Metal-complexing Agent: Synthesis, Characterization, and Metal (II) Ion Adsorption Studies. *Carbohydrate Research.* 345: 2013-2022.

[7] Wang, J., and Chen, C. 2014. Chitosan-based Biosorbents: Modification and Application for Biosorption of Heavy Metals and Radionuclides. *Bioresource Technology.* 160:129-141.

[8] Kyzas, G. Z., and Bikiaris, D. N. 2015. Recent Modifications of Chitosan for Adsorption Applications: A Critical and Systematic Review. *Marine Drugs.* 13: 312-337.

[9] Zhang, L., Zeng, Y. and Cheng, Z. 2016. Removal of Heavy Metal Ions Using Chitosan and Modified Chitosan: A Review. *Journal of Molecular Liquids.* 214:175-191.

[10] Guinesi, L. S., and Cavalheiro, E. T. G. 2006. Influence Of Some Reactional Parameters on the Substitution Degree of Biopolymeric Schiff Bases Prepared from Chitosan and Salicylaldehyde. *Carbohydrate Polymers.* 65: 557-561.

[11] de Araújo, E. L., Barbosa, H. F. G., Dockal, E. R. and Cavalheiro, É. T. G. 2017. Synthesis, Characterization and Biological Activity of Cu (II), Ni (II) and Zn (II) Complexes of Biopolymeric Schiff Bases of Salicylaldehydes and Chitosan. *International Journal of Biological Macromolecules.* 95: 168-176.

[12] Kocak, N., Sahin, M., Arslan, G., and Ucan, H. I. 2012. Synthesis of Crosslinked Chitosan Possessing Schiff Base and Its Use in Metal Removal. *Journal of Inorganic and Organometallic Polymers and Materials.* 22: 166-177.

[13] Kumar, M., Tripathi, B. P., and Shahi, V. K. 2009. Crosslinked Chitosan/Polyvinyl Alcohol Blend Beads for Removal and Recovery of Cd (Ii) From Wastewater. *Journal of Hazardous Materials.* 172: 1041-1048.

[14] Malladi, S., Isloor, A. M., Isloor, S., Akhila, D. S. and Fun, H. K. 2013. Synthesis, Characterization and Antibacterial Activity of Some New Pyrazole Based Schiff Bases. *Arabian Journal of Chemistry.* 6: 335-340.

[15] Nethaji, S., Sivasamy, A., Thennarasu, G. and Saravanan, S. 2010. Adsorption of Malachite Green Dye Onto Activated Carbon Derived from Borassus Aethiopum Flower Biomass. *Journal of Hazardous Materials.* 181: 271-280.

[16] Kandile, N. G., Mohamed, H. M., and Mohamed, M. I. 2015. New Heterocycle Modified Chitosan Adsorbent For Metal Ions (II) Removal from Aqueous Systems. *International Journal of Biological Macromolecules.* 72: 110-116.

[17] Borsagli, F. G. M., Mansur, A. A., Chagas, P., Oliveira, L. C. and Mansur, H. S. 2015. O-Carboxymethyl Functionalization of Chitosan: Complexation and Adsorption of Cd (II) and Cr (VI) as Heavy Metal Pollutant Ions. *Reactive and Functional Polymers.* 97: 37-47.

[18] Krishnapriya, K. R. and Kandaswamy, M. 2009. Synthesis and Characterization of a Crosslinked Chitosan Derivative with a Complexing Agent and Its Adsorption Studies Toward Metal (II) Ions. *Carbohydrate Research.* 344: 1632-1638.

[19] Li, N. and Bai, R. 2005. A Novel Amine-shielded Surface Cross-linking of Chitosan Hydrogel Beads for Enhanced Metal Adsorption Performance. *Industrial and Engineering Chemistry Research.* 44: 6692-6700.

[20] Cadogan, E. I., Lee, C. H. and Popuri, S. R. 2015. Facile Synthesis of Chitosan Derivatives and Arthrobacter Sp. Biomass for the Removal of Europium (III) Ions from Aqueous Solution Through Biosorption. *International Biodeterioration & Biodegradation.* 102: 286-297.

[21] Webster, A., Halling, M. D. and Grant, D. M. 2007. Metal Complexation of Chitosan and Its Glutaraldehyde Cross-Linked Derivative. *Carbohydrate Research.* 342: 1189-1201.

[22] Gunay, A., Arslankaya, E. and Tosun, I. 2007. Lead Removal from Aqueous Solution by Natural and Pretreated Clinoptilolite: Adsorption Equilibrium and Kinetics. *Journal of Hazardous Materials.* 146: 362-371.

[23] Bhatnagar, A. and Sillanpää, M. 2009. Applications of Chitin- and Chitosan-Derivatives for the Detoxification of Water and

Wastewater-A Short Review. *Advances in Colloid and Interface Science*. 152: 26-38.

[24] Foo, K. Y. and Hameed, B. H. 2010. Insights into the Modeling of Adsorption Isotherm Systems. *Chemical Engineering Journal*. 156: 2-10.

[25] Boddu, V. M., Abburi, K., Randolph, A. J. and Smith, E. D. 2012. Removal of Copper (II) and Nickel (II) Ions from Aqueous Solutions by a Composite Chitosan Biosorbent. *Separation Science and Technology*. 37-41.

[26] Qiu, H., Lv, L., Pan, B. C., Zhang, Q. J., Zhang, W. M. and Zhang, Q. X. 2009. Critical Review in Adsorption Kinetic Models. *Journal of Zhejiang University-Science A*. 10: 716-724.

[27] Ho, Y. S. and Mckay, G. 1999. Pseudo-Second Order Model for Sorption Processes. *Process Biochemistry*. 34: 451-465.

[28] Khan, A. A. and Singh, R. P. 1987. Adsorption Thermodynamics Of Carbofuran On Sn (IV) Arsenosilicate in H+, Na+ And Ca2+ Forms. *Colloids and Surfaces*. 24: 33-42.

[29] Yuvaraja, G., Yaping, Z., Weijiang, Z. and Jiao, X. 2017. Magnetic-epichlorohydrin Crosslinked Chitosan Schiff's Base (m-ECCSB) as a Novel Adsorbent for the Removal of Cu (II) Ions from Aqueous Environment. *International Journal of Biological Macromolecules*. 97: 85-98.